Noise Reduction in Drone Propellers: A Comparative Study of Design Optimization and Active Phase Control

Lukas Lübbert[1], Alessandro Fortino[1], Fevzi Kilic[1], Jonas Streppel[1]

[1]*Department of Mechanical Engineering, University of applied Sciences and arts, Germany*

Abstract

The rapid expansion of civilian drone applications has intensified concerns regarding environmental noise and its impact on human well-being. Due to their pronounced tonal and high-frequency components, drone noise is often perceived as particularly intrusive in urban environments, making noise reduction a key factor for public acceptance. This study investigates the acoustic characteristics of drone propellers and evaluates mitigation strategies combining passive design optimization and active noise control. Several propeller configurations, including toroidal designs and alternative blade geometries, are systematically compared to conventional two- blade propellers. A dedicated experimental test bench was developed to enable time-synchronous acquisition of acoustic and aerodynamic performance parameters, including sound pressure, electrical power consumption and thrust. This approach allows for a comprehensive, multi-criteria assessment of propeller performance. The results are analyzed with respect to trade-offs between noise emission aerodynamic efficiency, and thrust generation. In addition to passive design measures, active control strategies based on destructive interference are examined. In particular, phase shifts between multiple propellers and adaptive techniques targeting dominant tonal components are investigated. The findings demonstrate significant potential for reducing tonal noise while maintaining aerodynamic performance. The study provides insight into the optimization of drone propulsion systems and contributes to the development of quieter unmanned aerial vehicles for improved environmental compatibility.

Keywords: *Drone, Propeller, Noise, Synchrophasing*

Corresponding author: *lukas.luebbert@fh-dortmund.de*

1. Introduction

The use of unmanned aerial vehicles (UAVs) has expanded rapidly beyond military applications and now includes infrastructure inspection, precision agriculture, emergency response, aerial imaging, parcel delivery, and emerging concepts of urban air mobility.[1][2] As UAV operations increasingly move into populated environments, environmental noise has become a major challenge for public acceptance. [3][4]

Unlike conventional road traffic, the acoustic signature of multirotor UAVs is dominated by tonal components generated by the rotating propellers, particularly at the blade passing frequency (BPF) and its harmonics. [5] These tones are superimposed on broadband aerodynamic noise and have been shown to contribute disproportionately to perceived annoyance. [6] Consequently, reducing tonal propeller noise has become a primary objective in the development of low-noise UAV propulsion systems.

Two principal strategies are currently being pursued. Passive approaches reduce noise at the source through aerodynamic optimization of the propeller, for example by modifying blade geometry or employing toroidal designs.[7] While toroidal propellers have attracted considerable attention due to their potential to weaken tip vortices, reported acoustic benefits remain inconsistent when aerodynamic efficiency is considered simultaneously.[8] Active approaches, in contrast, exploit the coherence of the tonal emissions from neighboring propellers. By adjusting their relative phase angle, propeller synchrophasing enables constructive or destructive interference of the radiated sound field without altering the aerodynamic characteristics of the propulsion system.[9][10]

Although both approaches have received increasing attention, they are generally investigated independently. Furthermore, acoustic studies often do not provide a direct comparison of acoustic performance and propulsion efficiency under identical operating conditions. Consequently, direct experimental comparisons under identical operating

conditions remain limited.
To address this gap, a dedicated aeroacoustic test bench was developed that enables synchronized measurements of sound pressure, thrust, electrical power consumption, and rotational speed. Within this unified experimental framework, several conventional and toroidal propeller geometries are compared with respect to aerodynamic and acoustic performance, and the potential of active noise reduction through propeller synchrophasing is investigated using a dual-propeller configuration.
The objective of this work is to provide a direct experimental comparison of passive and active noise mitigation strategies and to assess their respective advantages and limitations for future low-noise multirotor propulsion systems.

2. Aeroacoustic Background

The acoustic emission of a rotating propeller is generated by periodically varying aerodynamic forces acting on the surrounding air. According to the Ffowcs Williams–Hawkings (FW–H) acoustic analogy, the radiated sound field can be attributed to three principal source mechanisms:[11]

- Thickness noise, caused by the displacement of air by the rotating blade volume,
- Loading noise, generated by unsteady aerodynamic forces acting on the blades, and
- Broadband noise, originating from turbulent boundary layers, tip-vortex interactions, and trailing-edge scattering. [12]

For electrically driven multirotor UAVs operating in hover, loading noise is the dominant contributor to the characteristic tonal acoustic signature. The most prominent tonal component occurs at the blade passing frequency (BPF), which is determined by the number of propeller blades and the rotational speed according to

$$f_{BPF} = N_b * \frac{n}{60} \tag{1}$$

where N_b denotes the number of propeller blades and n the rotational speed in revolutions per minute. For a representative operating point of 4000 1/min, the two-bladed reference propeller investigated in this study therefore exhibits a blade passing frequency of approximately 133 Hz.
Since the blade passing frequency and its higher harmonics dominate the perceived tonal character of UAV noise, they represent the primary target of both passive and active noise mitigation strategies investigated in this work.[13] Passive approaches aim to reduce the generation of tonal sound by modifying the aerodynamic properties of the propeller, whereas active synchrophasing seeks to attenuate these tonal components through controlled interference of multiple coherent sound sources.
Besides their acoustic performance, the investigated propellers are evaluated with respect to their aerodynamic efficiency. During each experiment, thrust, electrical current, and supply voltage are measured simultaneously, allowing the electrical input power to be calculated as

$$P_{el} = U \cdot I \tag{2}$$

To enable a direct comparison between different propeller geometries, the aerodynamic efficiency is expressed by the thrust-to-power ratio

$$\eta_T = \frac{T}{P_{el}} \tag{3}$$

where T denotes the generated thrust. This metric provides a practical measure of propulsion efficiency under hovering conditions and forms the basis for the multi-criteria evaluation presented in the following sections. To ensure a fair comparison, all investigated propellers are operated using the same brushless DC motor and electronic speed controller.

3. Experimental Setup

To enable a reproducible comparison of different propeller concepts, a dedicated aeroacoustic test bench was developed. The experimental setup allows the synchronized acquisition of aerodynamic and acoustic quantities under controlled laboratory conditions and forms the basis for all investigations presented in this work.

Figure 1. Aeroacoustic test bench for propeller design comparison.

The propulsion unit consists of a brushless DC motor driven by an electronic speed controller. The rotational speed is regulated by a closed-loop control system implemented in MATLAB/Simulink using a proportional–integral (PI) controller. This configuration enables precise and repeatable adjustment of the desired operating point over the complete measurement range.
The generated thrust is measured by means of a single-axis load cell mounted beneath the propulsion unit. Simultaneously, the electrical input power is determined from continuously recorded current and voltage signals. Together with the measured rotational speed, these quantities provide the basis for evaluating the aerodynamic performance of the investigated propeller geometries.

All acoustic measurements are carried out inside a semi-anechoic chamber using calibrated free-field microphones positioned at predefined measurement locations. The microphone arrangement and measurement distance are selected to ensure repeatable sound pressure measurements while minimizing the influence of reflections from surrounding structures. The synchronized acquisition of all measurement channels enables a direct correlation between aerodynamic operating conditions and the emitted acoustic field.

For the investigation of active noise reduction, the experimental setup is extended by a second, identical propulsion unit, resulting in a dual-propeller configuration. Both motors are equipped with incremental rotary encoders that provide continuous measurements of the instantaneous angular rotor positions. Based on these signals, a digital control algorithm synchronizes the rotational positions of both propellers and allows the relative phase angle to be adjusted with high accuracy. Consequently, the influence of constructive and destructive acoustic interference can be investigated under identical aerodynamic operating conditions.

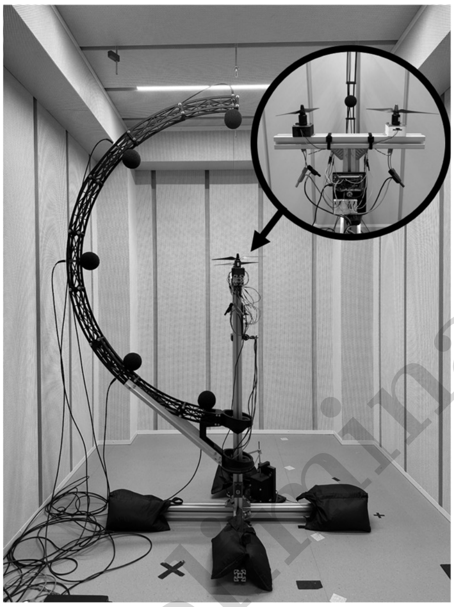

Figure 2. Aeroacoustic test bench for synchro phasing.

4. Passive Noise Reduction by Propeller Design

To investigate the influence of propeller geometry on aerodynamic and acoustic performance, several commercially available and additively manufactured propeller concepts were evaluated using the developed aeroacoustic test bench. The investigated designs included a conventional 280 mm two-blade propeller serving as the reference configuration, multiple toroidal propeller geometries of different diameters, and an alternative two-blade-geometry with a blade offset angle of approximately 55°. [7] [14][15][16] With the exception of the conventional reference propeller, all investigated geometries were manufactured using additive manufacturing.

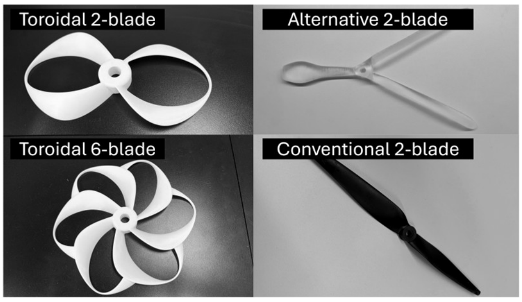

Figure 3. comparison of tested propeller designs.

Each propeller was characterized with respect to three evaluation criteria: generated thrust, electrical power consumption, and emitted sound pressure level (SPL). Measurements were conducted over a representative operating range covering typical hover conditions for small multirotor UAVs. This multi-parameter approach enables the simultaneous assessment of aerodynamic efficiency and acoustic performance.

Preliminary measurements revealed that the investigated alternative two-blade-geometry with an asymmetric blade offset angle exhibited considerable mechanical imbalance, resulting in elevated vibration levels and unstable acoustic behaviour. Since these effects are most likely related to manufacturing tolerances rather than the underlying aerodynamic concept, the design was excluded from the subsequent comparison. The following analysis therefore focuses on the conventional 280 mm two-blade reference propeller and two toroidal propeller geometries: a 280 mm two-blade design and a 200 mm six-blade toroidal design optimized for additive manufacturing.

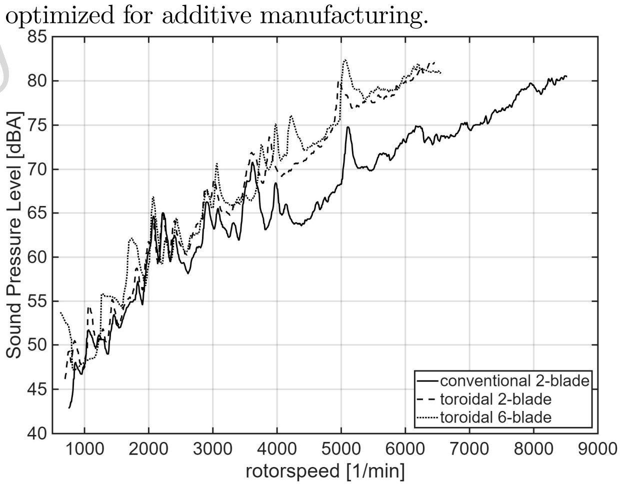

Figure 4. Sound pressure level as a function of rotorspeed.

Figure 4 presents the measured A-weighted sound pressure level as a function of rotational speed. For all investigated operating points, both toroidal propeller geometries exhibit higher measured overall sound pressure levels at the tested operating points than the conventional reference propeller. A similar trend can be observed when the sound pressure level is evaluated as a function of generated thrust, as shown in Figure 5. These results indicate that, for the investigated designs, the toroidal geometries do not provide a reduction in overall acoustic emission under comparable operating conditions.

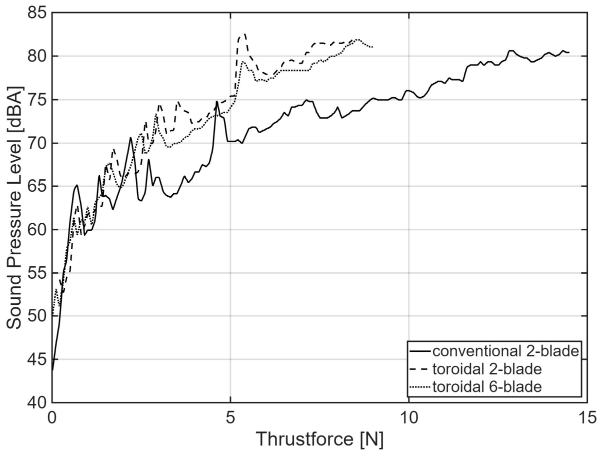

Figure 5. SPL as a function of generated thrust.

The measurements were limited to a maximum electrical input power of 180 W in order to prevent thermal overload of the propulsion system. Consequently, the maximum achievable thrust differed between the investigated propellers, leading to different end points in the performance curves. Based on the simultaneously measured thrust and electrical power consumption, the thrust-to-power ratio introduced in Section 2 was calculated for each propeller. The conventional reference propeller achieved a value of 0.080 N/W, whereas the investigated toroidal two-blade and six-blade geometries reached 0.046 N/W and 0.050 N/W, respectively. These results indicate that the investigated toroidal concepts exhibit a lower aerodynamic efficiency than the conventional reference design under the tested operating conditions.

While the overall sound pressure level favours the conventional propeller, a different picture emerges when considering the spectral composition of the emitted sound. Figure 6 compares the frequency spectra of the investigated propellers at a common operating point corresponding to a rotational speed of 3000 1/min. Although both toroidal geometries produce an elevated broadband noise floor, a pronounced reduction of the tonal blade passing frequency and its harmonics can be observed, particularly for the six-blade toroidal design.

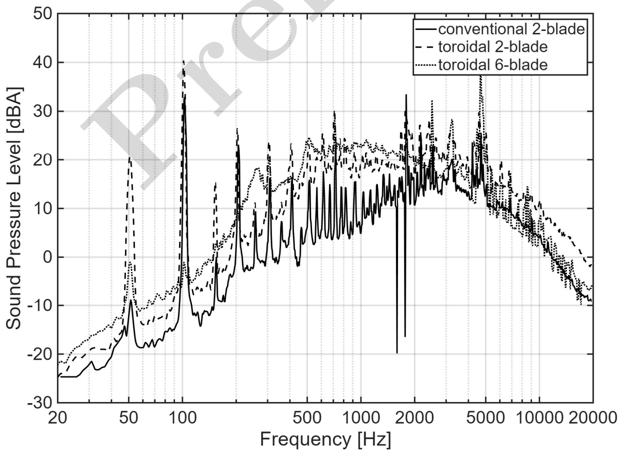

Figure 6. Propeller frequency spectra at 3000 1/min.

It should be noted that the investigated propellers generate different thrust levels at this operating point. At 3000 1/min, the conventional reference propeller produces approximately 1.19 N of thrust, whereas the toroidal two-blade and six-blade designs generate approximately 2.75 N and 1.33 N, respectively. Consequently, the higher spectral levels of the toroidal two-blade propeller must be interpreted in the context of its substantially increased aerodynamic loading. Nevertheless, the six-blade toroidal geometry exhibits a considerable attenuation of the dominant tonal components despite producing a comparable thrust level. This behaviour is likely related to the more continuous blade-tip geometry, which weakens the periodic loading fluctuations responsible for the tonal acoustic radiation.

Since the conventional reference propeller was manufactured using a different production process than the additively manufactured toroidal designs, the influence of manufacturing accuracy on the measured acoustic behaviour cannot be completely excluded. Future investigations should therefore include an additively manufactured replica of the conventional geometry to isolate manufacturing-related effects from purely geometric influences. Nevertheless, the investigated six-blade toroidal geometry demonstrated potential for reducing dominant tonal components of UAV noise, albeit at the expense of increased broadband noise and reduced aerodynamic efficiency. Overall, the measurements demonstrate that passive geometric optimization alone does not necessarily improve both aerodynamic and acoustic performance simultaneously and that significant trade-offs must be considered during propeller design.

5. Active Noise Reduction Using Synchrophasing

In addition to passive propeller optimization, active noise reduction was investigated using a dual-propeller configuration. The underlying principle is based on controlling the relative phase angle between two synchronized propellers. [17] Since both rotors emit highly coherent tonal sound at the blade passing frequency, adjusting their angular offset allows constructive or destructive interference to be generated at specific observation positions, thereby modifying the radiated sound field without altering the aerodynamic properties of the propulsion system. Because the interference pattern is spatially dependent, attenuation occurs only at specific observer locations. [18]

To realize this approach, both propulsion units were equipped with incremental rotary encoders providing continuous measurements of the instantaneous rotor positions. A digital master–slave control algorithm was implemented on an Arduino Mega to regulate the relative phase angle between the two propellers. Engine 1 serves as the master, while the rotational speed of Engine 2 is continuously adjusted such that the measured angular difference follows the prescribed reference phase angle. The controller operates by modifying the PWM command of the slave motor, thereby indirectly controlling its rotational speed. A schematic representation of the implemented control architecture is shown in Figure 7

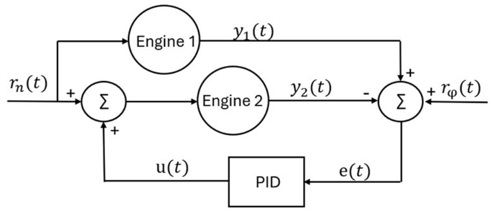

Figure 7. Implemented Master-Slave Control algorithm for synchrophasing

The developed control system achieves a phase accuracy of approximately ±5° for rotational speeds up to 4000 1/min. Since stable synchronization could be maintained throughout this operating range, all subsequent acoustic investigations were conducted at this rotational speed. The measurements presented in the following are based on two conventional two-blade propellers corresponding to the reference geometry introduced in the previous section.

To evaluate the influence of synchrophasing on the radiated sound field, acoustic measurements were performed for different prescribed phase angles and microphone positions. Figure 8 presents the average sound pressure spectrum obtained from all fifteen microphone positions. The uncontrolled case represents operation without phase synchronization, where the motor speeds are not actively matched and no specific phase relationship is imposed. While the overall sound pressure level remains nearly unchanged, only minor reductions of the dominant tonal components are observed in the spatially averaged data. The largest attenuation occurs at the blade passing frequency, where a phase angle of 90° reduces the tonal level by approximately 3 dB compared to the uncontrolled case. At the second harmonic, a phase angle of 45° yields an attenuation of approximately 2.5 dB. Overall, the averaged A-weighted sound pressure level is reduced by approximately 0.35 dB for the optimum phase angle.

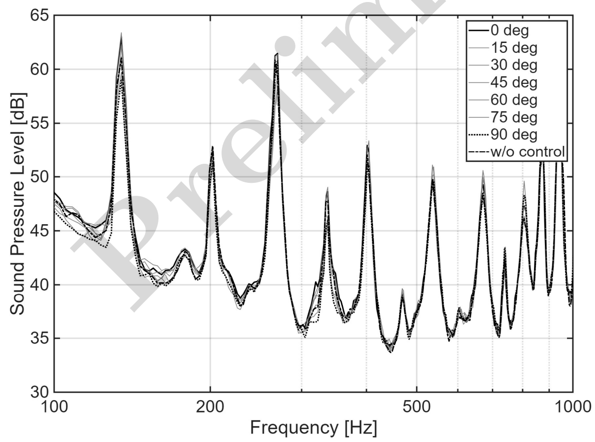

Figure 8. Influence of phase angle on average Sound pressure level over all positions.

A considerably stronger effect is observed when the sound pressure is evaluated at individual microphone positions. Figure 9 shows the spectrum measured within the propeller plane, where destructive interference is most pronounced. At the blade passing frequency, a phase angle of 90° results in an attenuation of approximately 15 dB compared with the uncontrolled case and approximately 18 dB compared with synchronized operation at 0°. At higher harmonics, the attenuation decreases significantly, indicating that synchrophasing is particularly effective for the dominant tonal component. Under these conditions, the overall sound pressure level is reduced by approximately 1.6 dB.

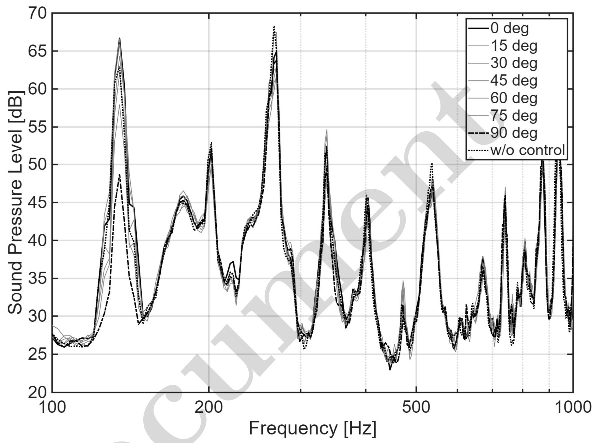

Figure 9. Influence of phase angle on Sound pressure level in Propeller plane.

Additional measurements performed at lower rotational speeds demonstrated even larger reductions of the blade passing frequency, reaching approximately 21 dB at 3000 1/min. However, since the primary operating range of multirotor UAVs corresponds to higher rotational speeds, the discussion is focused on the measurements conducted at 4000 1/min. The reduced effectiveness at higher rotational speeds can be attributed to the shorter acoustic wavelengths and the increased sensitivity of the interference pattern to small phase deviations.

The experimental results further highlight the directional nature of propeller synchrophasing. Rather than uniformly reducing the emitted acoustic energy, the controlled phase relationship redistributes the sound field, leading to substantial attenuation in some spatial directions while producing only minor changes in the spatially averaged sound pressure level. Consequently, the achievable noise reduction strongly depends on the observer position and the geometric arrangement of the propulsion system. [18]

Unlike passive geometric optimization, synchrophasing preserves the aerodynamic characteristics of the propulsion system because no modifications to the propeller geometry or operating point are required. Instead, it selectively targets the dominant tonal components through controlled interference of coherent sound sources.[18] These results demonstrate that synchrophasing represents a promising complementary approach to passive noise reduction, particularly for multirotor UAVs where several coherent acoustic sources are inherently available.

6. Discussion and Conclusions

The presented investigations demonstrate that passive and active noise mitigation strategies address different aspects of UAV aeroacoustics and should therefore be regarded as complementary. While passive propeller optimization modifies sound generation at the source, synchrophasing alters the radiated sound field through controlled interference of coherent tonal sources.

The investigated toroidal propeller geometries did not reduce the overall A-weighted sound pressure level and showed lower aerodynamic efficiency than the conventional reference propeller. However, spectral analysis revealed considerable attenuation of the blade passing frequency and its harmonics, particularly for the six-blade toroidal design. The results therefore indicate that these geometries primarily redistribute acoustic energy from tonal to broadband noise rather than reducing overall acoustic emission.

In contrast, synchrophasing substantially attenuated the dominant tonal components without affecting the aerodynamic operating conditions. Although only minor reductions in overall sound pressure level were observed, local attenuations of up to 15 dB at the blade passing frequency demonstrate the potential of active phase control for multirotor UAVs.

Overall, neither passive nor active noise mitigation alone provides a complete solution for reducing UAV noise emissions. Instead, both approaches address different physical mechanisms and can complement one another. Future work will investigate additional propeller geometries, manufacturing effects, and the extension of the synchrophasing strategy towards adaptive multi-propeller systems under realistic flight conditions.

References

[1] R. W. Beard and T. W. McLain, “Small Unmanned Aircraft: Theory and Practice”, Princeton, NJ: Princeton University Press, 2012.

[2] P. Fahlstrom and T. Gleason, Introduction to UAV Systems, 4th ed., Wiley, 2012.

[3] H Eißfeldt, V. Vogelpohl, “DRONE ACCEPTANCE AND NOISE CONCERNS - SOME FINDINGS “ In Proc. of the 20th Intern. Symp. on Aviation Psychology, 2019.

[4] National Academies of Sciences, Engineering, and Medicine, “Advancing Aerial Mobility: A National Blueprint”. Washington DC, National Academies Press, 2020.

[5] N. Intaratep, W. N. Alexander, W. J. Devenport, S. Grace, and J. Dropkin, "Experimental Study of Quadcopter Acoustics and Performance at Static Thrust Conditions," AIAA Journal, vol. 55, no. 12, pp. 4444–4457, 2016

[6] S. Torija and D. Clark, "A psychoacoustic approach to building knowledge about human response to noise of unmanned aerial vehicles," International Journal of Environmental Research and Public Health, vol. 18, 2021

[7] H. Jiang, H. Wu, W. Chen, P. Zhou, S. Zhong, X. Zhang, G. Zhou, and B. Chen, "Toward High-Efficiency Low-Noise Propellers: A Numerical and Experimental Study," Physics of Fluids, vol. 34, no. 7, Art. 076116, 2022.

[8] K. Bowers, S.J. Rovani, A. Samad, J. Hrynuk, H. Hu, Experimental Investigation on Aeroacoustic and Wake Flow Characteristics of Toroidal Propellers for Hybrid UAV Propulsion, AIAA AVIATION 2026 Forum, 2026

[9] B.B. Turhan, D. Rezgui, M. Azarpeyvand, Acoustic Effects of Differential Rotor Speeds on Twin-Propeller UAV System, Drones 2026, 10(4), mdpi, 2026

[10] Z, Yang, M. Meinke, D. Krug, W. Schröder , " Numerical Investigation on Noise Reduction of Distributed Propellers by Phase Synchronization," Forum Acusticum Euronoise, Malaga, Spain, 2025

[11] J. E. Ffowcs Williams and D. L. Hawkings, "Sound Generation by Turbulence and Surfaces in Arbitrary Motion," Philosophical Transactions of the Royal Society of London A, vol. 264, 1969

[12] F. Farassat, "Derivation of Formulations 1 and 1A of Farassat", NASA Technical Memorandum 2007-214853, 2007

[13] G. Huang, A. Sharma, X. Chen, A. Riaz, and R. Jefferson-Loveday, "Numerical Predictions of Low-Reynolds-Number Propeller Aeroacoustics: Comparison of Methods at Different Fidelity Levels," Aerospace, vol. 12, no. 2, Art. 154, 2025.

[14] D. Usov, D. Koning, T. Chronis, A. Filippone, D. Akiwate, A. J. T. Martinez; “Aerodynamics and Acoustics of Asymmetric Propellers With Uneven Blade Spacing”, 30th AIAA/CEAS Aeroacoustics Conf., Rome, Italy,2024

[15] B. J. D. Wade, "Reduced noise rotor for aerial vehicles", US Patent No 12,649,591, 2026

[16] S. Prakhar, J.-H. Seo, and R. Mittal, "Aeroacoustics of Unconventional Drone Rotors – From Leonardo da Vinci's Designs to Toroidal Loops," 76th Annual Meeting of the APS Division of Fluid Dynamics, Washington DC, 2023

[17] B. Turhan, H. K. Jawahar, A. Gautam, S. Syed, G. Vakil, D. Rezgui, M. Azarpeyvand, "Acoustic characteristics of phase-synchronized adjacent propellers," The Journal of the Acoustical Society of America, vol. 155, no. 5, pp. 3242–3253, 2024.

[18] F. do Nascimento Monteiro, R. R. Duivenvoorden, D. Ragni, T. Sinnige, and F. Avallone, "Experimental Analysis of Synchrophasing Impact on Noise of Distributed Propeller Systems in Tractor Configuration," in Proc. of the 30th AIAA/CEAS Aeroacoustics Conference, 2024.